Clim Dyn
DOI 10.1007/s00382-016-3222-4

How predictable is the winter extremely cold days over temperate East Asia?

Xiao Luo[1,2] · **Bin Wang**[2,3]

Received: 18 December 2015 / Accepted: 3 June 2016

Abstract Skillful seasonal prediction of the number of extremely cold day (NECD) has considerable benefits for climate risk management and economic planning. Yet, predictability of NECD associated with East Asia winter monsoon remains largely unexplored. The present work estimates the NECD predictability in temperate East Asia (TEA, 30°–50°N, 110°–140°E) where the current dynamical models exhibit limited prediction skill. We show that about 50 % of the total variance of the NECD in TEA region is likely predictable, which is estimated by using a physics-based empirical (P-E) model with three consequential autumn predictors, i.e., developing El Niño/La Niña, Eurasian Arctic Ocean temperature anomalies, and geopotential height anomalies over northern and eastern Asia. We find that the barotropic geopotential height anomaly over Asia can persist from autumn to winter, thereby serving as a predictor for winter NECD. Further analysis reveals that the sources of the NECD predictability and the physical basis for prediction of NECD are essentially the same as those for prediction of winter mean temperature over the same region. This finding implies that forecasting seasonal mean temperature can provide useful information for prediction of extreme cold events. Interpretation of the lead–lag linkages between the three predictors and the predictand is provided for stimulating further studies.

Keywords Climate predictability · Prediction of extremely cold events · East Asia winter monsoon (EAWM) · El Niño/La Niña · Arctic Ocean temperature anomalies

1 Introduction

Extremely cold events have profound influences on people's livelihoods and economy in East Asian countries such as China, Japan, and Korea. There has been an increasing societal demand for seasonal forecast of the number of extreme events such as ECD. For instance, the policymakers need the information to decide their budget for heating costs. Transportation industry needs it to plan the amount of fuel to be transported. Planning agricultural activity also needs the forecasted frequency of NECD and mean temperature. Accurate forecast of winter mean temperature and NECD will greatly benefit policymakers and stackholders. Seasonal prediction of the frequency of extremely cold day (ECD) occurrence and estimation of its predictability has been one of frontier challenge in climate science.

Geographically, the present study focuses on temperate East Asia (TEA, 30°–50°N, 110°–140°E), the "heart" of EAWM. The TEA region is located in between the Aleutian low and Mongolian-Siberian High and underneath the southern part of the EA trough with the prevailing surface northerlies, a region which is closely associated with three main components of EAWM circulation system (Fig. 1). Furthermore, this densely populated TEA region is home to variety of modern industries and has strong demands for accurate forecast of extremely cold events.

✉ Bin Wang
Wangbin@hawaii.edu

[1] School of Atmospheric Sciences, Nanjing University, Nanjing 210023, China

[2] Department of Atmospheric Sciences and Atmosphere-Ocean Research Center, University of Hawaii at Manoa, Honolulu, HI 96822, USA

[3] Earth System Modeling Center, Nanjing University of Information Science and Technology, Nanjing 210044, China

Published online: 08 July 2016

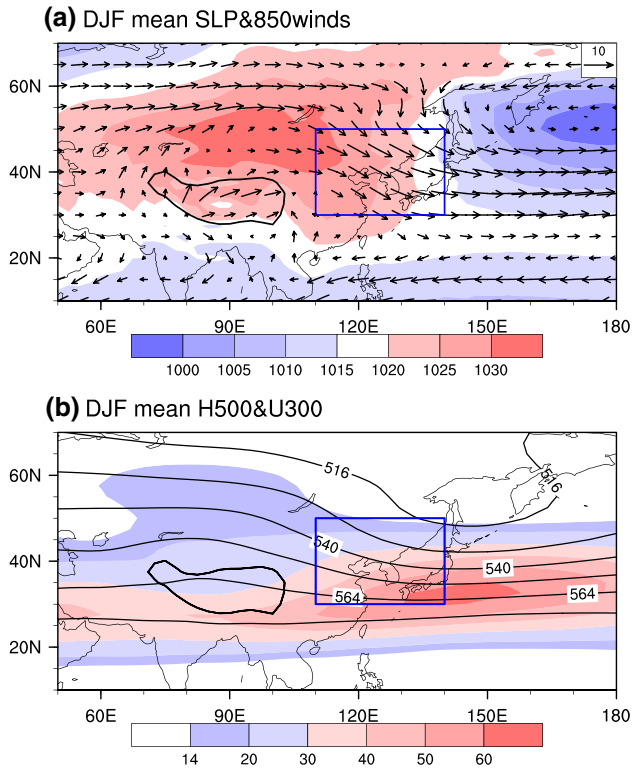

Fig. 1 Winter (DJF) mean circulations in the domain of Asian winter monsoon. **a** Sea-level pressure (SLP; *shaded*; hPa) and 850 hPa winds (*vectors*; m s^{-1}), **b** 500 hPa geopotential height (*contours*; 10 gpm) and 300 hPa zonal wind (*shaded*; m s^{-1}). The 3000 m topographic contour outlines the location of the Tibetan Plateau. The *boxed region* (30°–50°N, 110°–140°E) at each *panel* indicates the location of temperate East Asia (TEA)

Substantial effort has been made in understanding seasonal mean temperature variability over East Asia, which provides clues for seasonal prediction of extreme cold events. Variety of factors controlling EA winter temperature variations have been found, including El Niño/Southern Oscillation (ENSO) events (Zhang et al. 1996; Wang et al. 2000), Arctic sea ice anomaly (Honda et al. 2009; Kug et al. 2015), Eurasian snow cover anomalies (Clark and Serreze 2000; Watanabe and Nitta 1999; Wang et al. 2010), and sea surface temperature anomalies over Indian Ocean and North Atlantic (Wang et al. 2010; Wang and Chen 2014; Liu et al. 2014) in the preceding autumn.

Despite considerable progress made in understanding the sources of climate variability, prediction of the seasonal mean temperature over EAWM remains an outstanding and challenging task in climate science (Wang et al. 2009a; Lee et al. 2013). How skillful are the current dynamical models' predictions of the winter mean temperature over the TEA region? To answer this question, we have assessed the performance of the 46-year (1960–2005) retrospective forecast made by five models that participated in ENSEMBLE project (Weisheimer et al. 2009), and found that the multi-model ensemble hindcast yielded a domain-averaged temporal correlation skill of 0.29 for the TEA region (figure not shown), which is significant but rather limited.

Seasonal prediction of the extreme cold conditions has been a rare practice and presumably more difficult than seasonal mean temperature prediction due to its infrequent occurrence. For prediction of the extreme cold condition, ENSO has been recognized as the most important factor on the global scale (Pepler et al. 2015; Hamilton et al. 2012), but in many regions forecast of extreme temperatures can still be skillful even if ENSO effect is removed (Pepler et al. 2015). Therefore, for the TEA region, what role does ENSO play in determining ECDs in the TEA region? Besides ENSO, would any other physically consequential precursors exist?

Capability of dynamical models in seasonal prediction of extreme events was assessed only in the past few years. Hamilton et al. (2012) showed that the correlations of predicted and observed numbers of extreme days over a season are significantly greater than zero over much of the globe and dynamical prediction is generally better than persistence forecast. Using UK Met Office seasonal forecasting models, Eade et al. (2012) found that the multi-model ensemble (MME) prediction of winter extremes obtained an average correlation skill of 0.28 over global land. Pepler et al. (2015) have shown that the skill of a multi-model ensemble in forecasting 10th percentile of daily minimum temperature is statistically insignificant over mid- and low-latitude East Asia.

Apart from the dynamical models' evaluation, the exploration of the potential predictability and prediction of ECD has been rare so far. Considering the deficiencies of dynamical models in predicting ECD, to what extent we can predict the extreme cold winter days remains unanswered and the physical basis for such a prediction and the sources of predictability remain elusive.

In the present study, we aimed to explore the predictability sources and limits for the frequency of ECD over a season in the TEA region. Although dynamical seasonal prediction is an ultimate tool for seasonal forecast, in view of their limited skills at present, we will use physics-based empirical (P-E) model approach to understand the sources and estimate limits of predictability of NECD. This approach has been effectively applied to study Indian and East Asian summer rainfall prediction (Wang et al. 2015; Xing et al. 2014; Li and Wang 2015; Yim et al. 2014). Section 2 describes the datasets and methodology. Section 3 defines the ECD and the predictand. Section 4 presents characteristics of NECD-related simultaneous circulation anomalies. In Sect. 5, we search for physically consequential predictors and followed by establishing a P-E model to estimate the predictability of NECD in

Sect. 6. Section 7 presents shared sources of predictability between the winter mean temperature and the extreme cold conditions. The last section summarizes major results.

2 Data and methodology

2.1 Data

This study uses daily and monthly circulation data from the National Centers for Environmental Prediction-National Center for the Atmospheric Research (NCEP-NCAR) reanalysis (Kalnay et al. 1996). The time period analyzed in this study is 41 winters from 1973/1974 to 2013/2014. For simplicity, the winter of 1973 refers to the December 1973 to February 1974. The sea surface temperature (SST) data gridded at 2° × 2° resolution is derived from the National Oceanic and Atmospheric Administration (NOAA) extended reconstructed SST (ERSST version 3b) (Smith et al. 2008) for the same period. In addition, monthly mean precipitation are adopted from Global Precipitation Climatology Project (GPCP) version 2.2 dataset for the period of 1979–2013 (Huffman and Bolvin 2011).

To assess the performance of the dynamical models, we used retrospective forecasts made by the ENSEMBLES project for the period of 1960–2005 (Weisheimer et al. 2009). This data set consists of five state-of-the-art coupled atmosphere ocean circulation models, i.e., the Euro-Mediterranean Center for Climate Change (CMCC-INGV) in Bologna, European Centre for Medium-Range Weather Forecasts (ECMWF), the Leibniz Institute of Marine Sciences at Kiel University (IFM-GEOMAR), Météo France (MF), and UK Met Office (UKMO). The hindcasts were initiated form Nov. 1st that yielded a 1-month-lead DJF forecast. The MME prediction was made by simply averaging the above five models' predictions.

2.2 Method

Distinguished from pure statistical model, the P-E model aims to identify the most consequential predictors based on understanding of the physical processes that explain the lead–lag relationships between predictors and the predictand (Wang et al. 2015). Statistical methods are used as an auxiliary tool to maximize the predictors-predictand correlation in training periods.

To search for physically meaningful predictors, we focus on only three fields that reflect ocean and land surface anomalous conditions: (a) sea surface temperature (SST) over oceans and 2 m air temperature (T2m) over land, the latter often reflects snow cover anomalies, (b) sea level pressure (SLP) and (c) 500 hPa geopotential height. Meanwhile, we focus on two types of precursors, i.e., the persistent signals in autumn represented by the mean of September–October–November (SON) and tendency signal across autumn from September to November (November minus September). These persistent and tendency signals can reflect atmosphere–ocean–land interaction processes and indicate the maintenance of the anomalies and direction of its development, respectively. Long-term trend estimated by the least squares method can be found in seasonal mean fields, especially Arctic Ocean temperature in autumn (figures not shown). Since the trend could be due to external forcing or governed by different mechanisms than those governing natural interannual and decadal variation, we removed the linear trends from all the seasonal mean fields, based on 41 samples (1973–2013).

To circumvent over-fitting, the number of predictors is limited to three (i.e., <10 % of the sample size of 40). The prediction model is derived by stepwise multi-linear regression. All the predictor variables are normalized and selected at 95 % statistical significance level according to Fisher's F-test.

In addition, cross-validation method is employed to make a retrospective forecast (Michaelsen 1987). We train the model with the sample leaving 3 years out each time, and then apply the derived model to forecast the middle year of the three withheld years.

3 Definition of ECD and the predictand-NECD

A number of indices have been developed to quantify the ECD. The "Day-count" indices use fixed thresholds, which are less suitable for regions that exhibit large spatial variation (Zhang et al. 2011). In particular, a temperature threshold that is good for representing extremely cold days in mid-latitudes can only indicate a mild winter day at higher latitudes. Indices based on the count of days crossing percentile thresholds can provide useful local information for the impact and adaption. For instance, the indices of cold nights (TN10P) defined by experts of the CCI/CLIVAR/JCOMM Team on Climate Change Detection and Indices (ETCCDI), i.e., the number of days with daily minimum temperature below the 10th percentile of daily minimum temperatures (Zhang and Yang 2004), are relevant for comparing changes in heating demands (Zhang et al. 2011; Frich et al. 2002; Klein Tank et al. 2009). Some other indices such as cooling degree days and heating degree days, defined by the daily difference between mean temperature and a base temperature, are typical indicators of household energy consumption for space heating/cooling (Arguez et al. 2012), which are widely used for monitoring energy consumption.

In the present study, the threshold used to define ECDs is the 10th percentile of daily mean temperature. Instead of

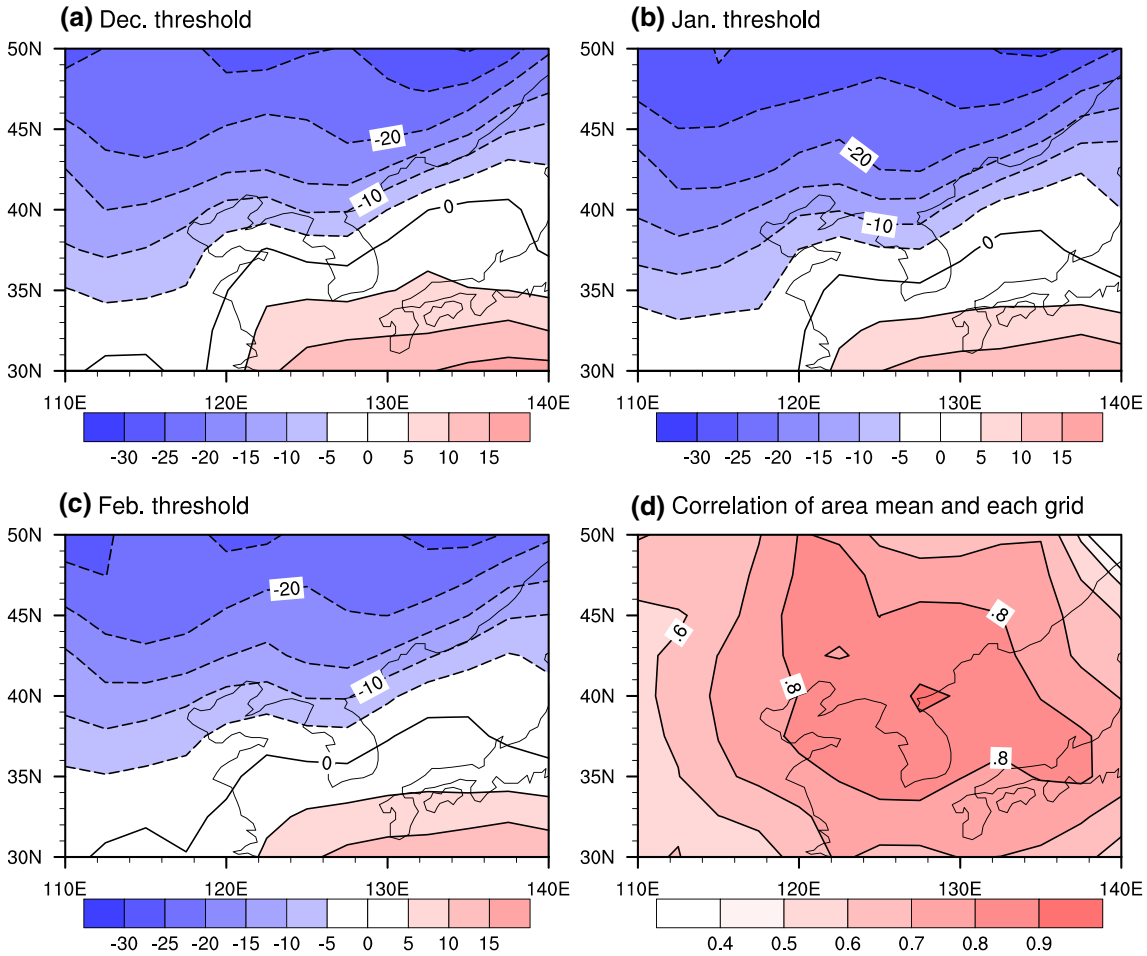

Fig. 2 Definition of extremely cold days. **a**–**c** Thresholds values (°C) defined for the extreme cold days (ECDs) over TEA, which are 10th percentile of daily mean temperature within the month of **a** December, **b** January, and **c** February. **d** Map of correlation coefficients between the areal averaged number of ECD (NECD) over TEA and the number of winter ECDs at each grid point

using a constant seasonal threshold, we calculated threshold values at each grid point over the TEA region and for each winter month from December to the following February. As shown in Fig. 2a–c, the threshold values vary moderately from December to February: The area-mean 10th percentile thresholds over the entire TEA region are −8.4 °C for December, −10.6 °C for January, and −8.6 °C for February. Spatially, the thresholds generally decrease from southeast to northwest across the TEA domain. The 0 °C threshold line is located over Sea of Japan, South Korea and the Yellow Sea, and reaches its southernmost point in January. The −25 °C threshold line migrates to 45°N in January and retreats to the northern boundary (around 50°N) in December and February.

For each grid point, an accumulative number of the ECDs during winter season (December, January and February, or DJF) can deliver useful local information. However, in order to simplify the prediction study, we do not deal with the accumulated ECDs at each grid. Rather, we aim to predict the number of ECDs (NECD) averaged over the entire TEA region. Thus, the predictand, NECD, is obtained by first summation of the accumulative number of winter ECDs at all grid points over TEA region and then divided by the total number of grids.

How does this area-mean predictand represent local information at each grid? As shown in Fig. 2d, the NECD generally well represents the numbers of ECDs over majority of the grids except in the northeast and southwest corners of the TEA domain as evidenced by the significant correlation coefficients exceeding 0.7. Therefore, NECD is a meaningful predictand not only for domain average but also for most grid points in TEA.

Figure 3 shows the time series of the NECD over the TEA region during 1973–2013 without removing the linear trend. Surprisingly, the trend in NECD was only −0.7 % per decade during the recent 41 years, which is insignificant according to Mann–Kendall test (Mann 1945; Kendall 1975). The time series of the NECD feature large

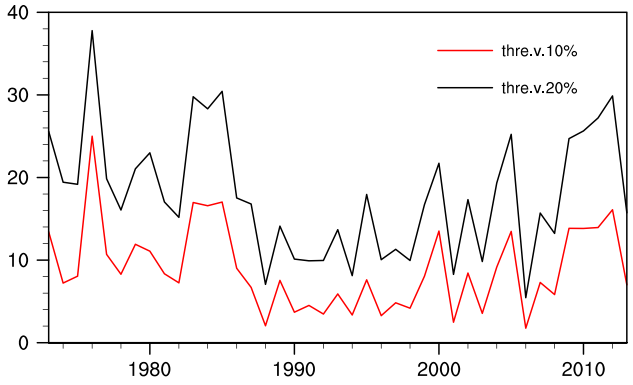

Fig. 3 Time series of the areal mean number of extremely cold days during winter over the TEA defined by 20th (*black line*) and 10th (*red line*) percentile of daily mean temperature for 1973–2013

year-to-year fluctuations and decadal variations. Large NECD years can be found in the period before mid-1980s, whilst low NECD years persist from the late 1980s to the early 2000s. After the early 2000s, there is an upward swing in the NECD with amplified year-to-year variability.

In the present study, our target is to estimate the predictability of the domain-averaged number of the 10th percentile ECDs over the TEA region. We denote this predictand specifically as NECD over the TEA region or simply NECD.

4 Circulation anomalies associated with NECD over the TEA region

It is a natural starting point to find out what the major circulation anomalies are when more ECDs occur in the TEA region. Figure 4 shows that more frequent occurrence of ECD in TEA region implies a continental scale cold winter covering the entire North and East Asia (Fig. 4a). This large scale cold winter is linked to a prominent anomalous high sea-level pressure (SLP) over northern Ural mountain and an anomalous low SLP to the east of Japan, indicating a northwestward migration of the Mongolian-Siberian High and a southwestward shift of the Aleutian Low, respectively (Fig. 4b). On the 500 hPa level, negative geopotential height anomalies are observed over northeast China and eastern Mongolia (Fig. 4c), indicating an enhancement and southwestward displacement of mid-tropospheric East Asian trough that normally extends from Okhotsk Sea to Yangtze River delta (Fig. 1b). A positive 500 hPa height anomaly occurring over northern Ural Mountain (Fig. 4c) indicates enhancement of the Ural Mountain ridge. Correspondingly, the zonal wind at 300 hPa accelerates over Northern China and weakens over southern Siberia (Fig. 4d), implying a northward shift of subtropical

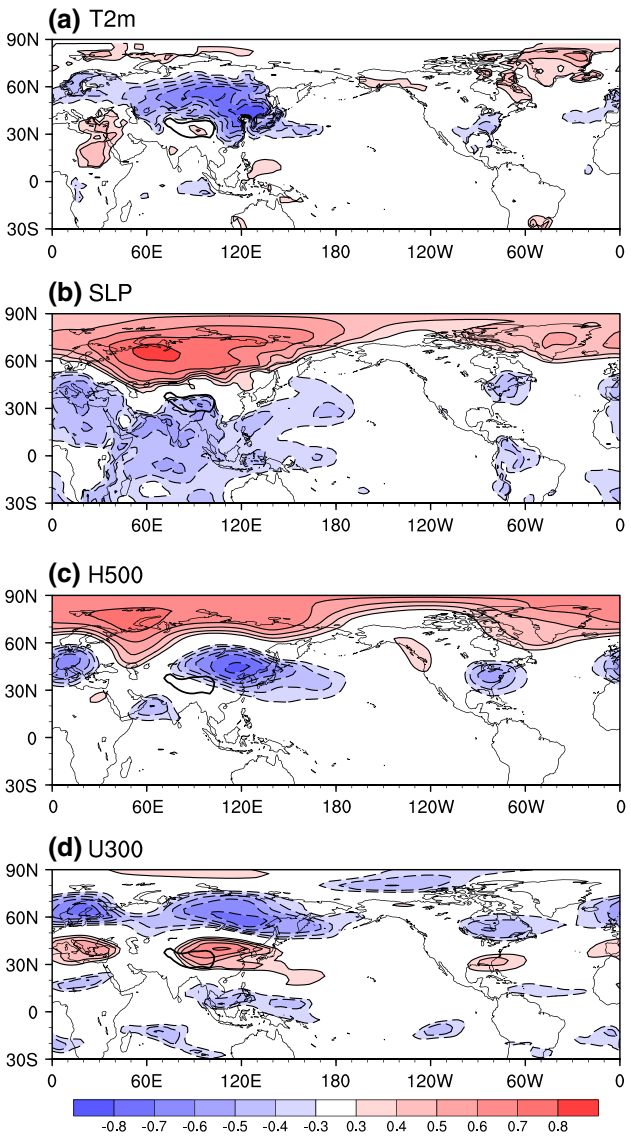

Fig. 4 Winter (DJF) temperature and circulation anomalies associated with the NECD over TEA. Shown are the concurrent correlation maps between the NECD over TEA and **a** 2 m air temperature (T2m) over land and SST over oceans, **b** SLP, **c** 500 hPa geopotential (H500), and **d** 300 hPa zonal wind (U300). *Shadings* indicate the regions with correlations significant at 95 % confidence level

westerlies and a southeastward migration of mid-latitude westerlies associated with the Asian polar front jet that normally located to the west of Lake Baikal (Fig. 1b). Note that these circulation anomalies resemble those associated with the so-called "northern mode" of a cold East Asian winter monsoon (Wang et al. 2010; Luo and Zhang 2015). These anomalies also suggest that an increased number of ECDs may be associated with a negative phase of Arctic Oscillation (AO), and the correlation coefficient between AO index (Thompson and Wallace 1998) and NECD is −0.64, significant at 99 % confidence level.

5 Predictors for winter NECD

5.1 Searching for predictors

To understand the sources of predictability we begin with exploration of predictors. Based on the previous studies and physical consideration discussed in Sect. 2, we restrict the search for predictors to the preceding autumn (SON) mean and tendency (November minus September) of three fields: surface temperature (SST/T2m), SLP and 500 hPa geopotential height (H500). Search for potential predictors are based on lead correlation coefficient (LCC) maps of the potential predictor fields with reference to the winter NECD. Attention is paid to large-scale coherent LCC regions where the correlation is statistically significant at 95 % confidence level.

In the LCC map of autumn mean SST/T2m field, coherent and significant LCC regions are seen in Eurasian Arctic Ocean (Fig. 5a). The warming in the Arctic region captures the signals from the polar region, which is the permanent source of the cold air. Since in September and October Arctic Ocean has minimum sea ice concentration, we used September–October mean SST anomalies averaged over Eurasian Arctic region (70°N–85°N, 25°E–140°E) as a potential predictor and named it as ARC-SST. There are some precursory signals in the North Pacific, but they are not independent from tropical Pacific tendency signals discussed in the next paragraph.

In the LCC map of the SST/T2m tendency field (Fig. 5b), significant LCC region is seen in the tropical Pacific, in particular the decreasing SST in equatorial eastern Pacific and rising SST in the equatorial western Pacific. This zonal dipolar SST tendency implies a developing La Niña condition across the preceding autumn. Therefore, we select the east–west Pacific dipolar SST tendency (November minus September) as second potential predictor, named ENSO- DSST (Fig. 5b; Table 1).

In the LCC map of the H500 field (Fig. 5c), prominent LCC regions are found over Asian sector: high anomalies over northern Asia-Arctic region and low anomalies over East Asia. To reflect this north–south dipolar pattern, we select the north–south dipolar height anomaly over East Asia as another potential predictor and named EA-H500 (Fig. 5c; Table 1). In other LCC maps (SLP mean and tendency and H500 tendency fields), no large-scale, coherent and statistically significant precursors are found. Note also that the selected three predictors likely represent distinctive physical processes that link to EAWM and the NECD in the TEA region. In fact, the mutual correlation coefficients among the three predictors are all statistically insignificant, except for the correlation coefficient between ENSO-DSST and ARC-SST, as shown in Table 2.

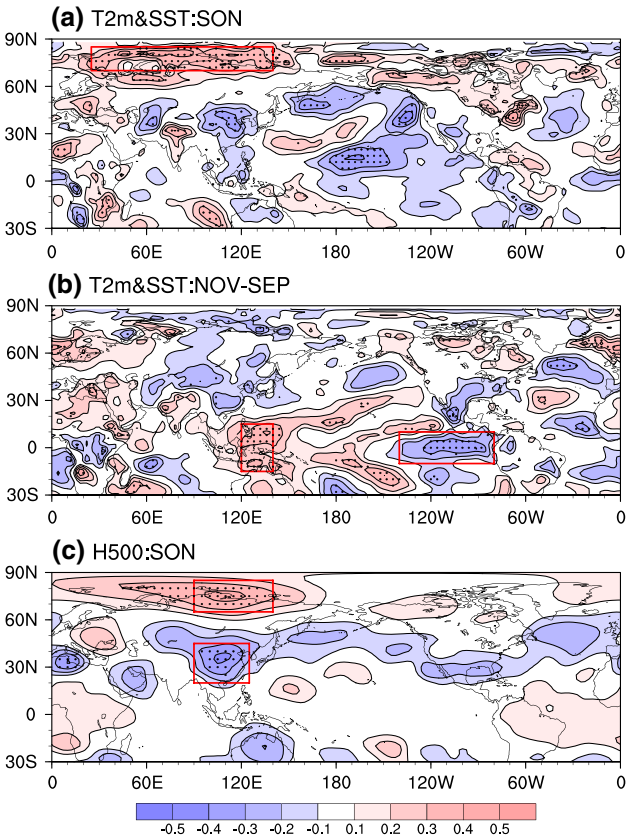

Fig. 5 Fall precursory anomalies associated with winter NECD over TEA. **a** Correlation maps of NECD and SON (September–October–November) mean SST over ocean and T2m over land, **b** same as (**a**), but for November minus September (tendency) SST/T2m, and **c** same as (**a**), but for SON mean H500. *Black dots* represent the regions with correlation significant at 95 % level. The *rectangular boxes* in each *panel* outline the regions where predictors are defined (Table 1)

5.2 Physical interpretations of the predictors

In establishing P-E model, it is important to understand how the selected predictors possibly link to the predictand. For this purpose, we examine winter mean anomalies associated with the selected predictor using the anomaly maps that are regressed with reference to the selected predictors. The regressed winter anomalies are considered as associated with the autumn predictor. In the following we discuss how the ARC-SST, ENSO-DSST, and EA-H500 related to the associated winter NECD anomaly, respectively.

The Arctic SST and sea ice concentration as well as the surface air temperature are closely related to each other, thus the autumn ARC-SST predictor is capable of capturing the anomalous boundary conditions in the northern polar region. The Eurasian Arctic warming in September and October may persist into the next winter due to large ocean heat capacity, causing Arctic Ocean warmth in winter (Fig. 6a). As shown by the numerical experiments made

Table 1 Definition of selected predictors for prediction of NECD

Name	Definition	
ARC-SST	Sep. and Oct. mean	SST (70°N–85°N, 25°E–140°E)
ENSO-DSST	Nov. minus Sep.	DSST (10°S–10°N, 80°W–130°W)–DSST (15°S–15°N, 120°E–140°E)
EA-H500	SON	H500 (20°N–45°N, 90°E–125°E)–H500 (65°N–85°N, 90°E–140°E)

Table 2 The correlation coefficients between NECD and predictors and between any two of the predictors during 1973–2013

	NECD	ENSO-DSST	ARC-SST	EA-H500
NECD		**−0.56**	**0.58**	**−0.49**
ENSO-DSST			*−0.39*	0.19
ARC-SST				−0.10
EA-H500				

The bold (italic) numbers denote statistically significant at 99 % (95 %) confidence level

by Kug et al. (2015), the winter Arctic warming, especially over the Kara Sea, can induce an anticyclonic anomaly extending from polar region to Ural Mountain, which is seen from surface up to 500 hPa (Fig. 6a, b). The rising pressure over Ural Mountain can further lead to downstream low pressure anomalies that deepen and shift westward the East Asian trough at 500 hPa (Fig. 6b) through Rossby wave propagation (Kug et al. 2015). It has been well documented that the rising pressure over Ural mountain region and deepening EA trough favor for more frequent occurrence of cold surges over TEA (Chang et al. 2006, also Fig. 4c).

How does the ENSO-SST predictor lead to a more frequent occurrence of ECD during winter? The Eastern Pacific cooling-western Pacific warming tendency in autumn foreshadows a positive Bjerknes feedback between zonal SST gradient, zonal wind stress and upwelling (Wang et al. 2015), leading to a mature phase of La Niña during the following winter (Fig. 7a). A large scale cyclonic wind anomaly (with two centers located at Philippines and east of Japan, respectively) appears over western North Pacific associated with mature phase of La Niña (Fig. 7a), which is the counterpart of the western North Pacific anticyclone during El Niño phase (Wang et al. 2000). The northerly anomaly induced by the anomalous cyclone over western North Pacific at midlatitude EA facilitates cold air intrusion into to the TEA region. During La Niña events, cold SST in the eastern-central Pacific generates low-level equatorial easterly anomalies and enhances the precipitation heating over the Maritime Continent (Fig. 7b), which further strengthens upward motion over the maritime continent and the associated northward divergent winds at upper level (Fig. 7b). As a result, the upper tropospheric westerly over the northern (southern) part of the subtropical (polar front) jet is accelerated due to Earth's rotation as evidenced by zonal wind anomaly at 300 hPa (Fig. 7b), suggesting the impact of ENSO through the meridional overturning mechanism. Moreover, a meridional wave train over East Asia is associated with anomalous northward propagation of wave activity flux (Fig. 7c), thus deepening the EA trough as shown by the 500 hPa height anomaly (Fig. 7c). Circulation anomaly associated with the meridional teleconnection modulate the upper zonal winds that lead to reduced westerly in the mid-high latitude (60°N), and accelerated zonal wind in mid latitude (35°N) over East Asia. There is another zonal Eurasian wave train that links to EA trough but origin of the east–west Eurasian wave train remains elusive, which is unlikely related to ENSO directly. These distinct features associated with ENSO-DSST predictor signify circulation anomalies that lead to a more frequent ECD occurring over TEA (Fig. 4). An opposite SST tendency across equatorial Pacific leads to a mature El Niño, which tends to have reversed circulation anomalies and opposite effects on East Asian winter monsoon and NECD.

The EA-H500 is not a direct lower boundary anomaly. However, careful inspection of the autumn anomaly shown in Fig. 5 reveals that the 500 hPa height anomalies over the Asian sector, i.e., the Asian Arctic high and East Asian low anomalies (Fig. 5c), are closely linked to the lower boundary temperature anomalies, namely the anomalous warmth over Asian Arctic and the anomalous cooling over East Asia, respectively (Fig. 5a). Therefore, the 500 hPa height anomalies associated with EA-H500, to a large extent, are rooted in the surface anomalous thermal conditions and exhibit a deep equivalent barotropic structure. Further analysis shows the correlation coefficient between winter the North Atlantic Oscillation (NAO) index and EA-H500 is −0.40, which is significant 99 % confidence level (Barnston and Livezey 1987). It implies EA-H500 predictor may carry information of NAO signal, which is associated changes of surface temperature and snow cover over the Eurasian continent, and may affect EAWM through thermal advection (Watanabe 2004; Watanabe and Nitta 1999; Gong et al. 2002; Jhun and Lee 2004). Comparison of Figs. 5c and 8 unravels that the 500 hPa low

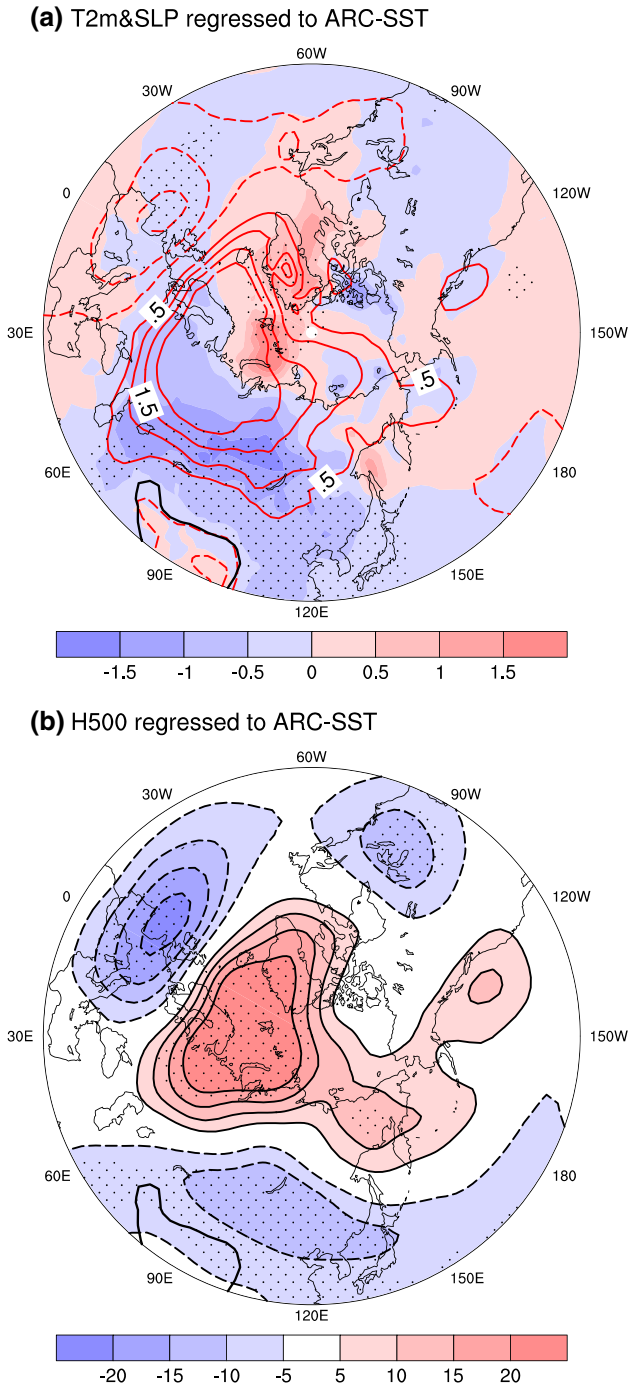

Fig. 6 Winter circulation anomalies associated with the autumn ARC-SST predictor. **a** The regressed winter SLP (*contours*; hPa) and T2m (*shaded*; °C) anomalies with reference to autumn ARC-SST predictor. The contour interval is 0.5 hPa and positive (negative) contours are *solid* (*dashed*) *lines*. The zero contour is not shown. **b** Same as (**a**), but for the 500 hPa height anomalies (*shaded*; gpm). *Dots* in (**a**) and (**b**) indicate regressed anomalies of T2m and 500 hPa geopotential height significant at 95 % confidence level, respectively

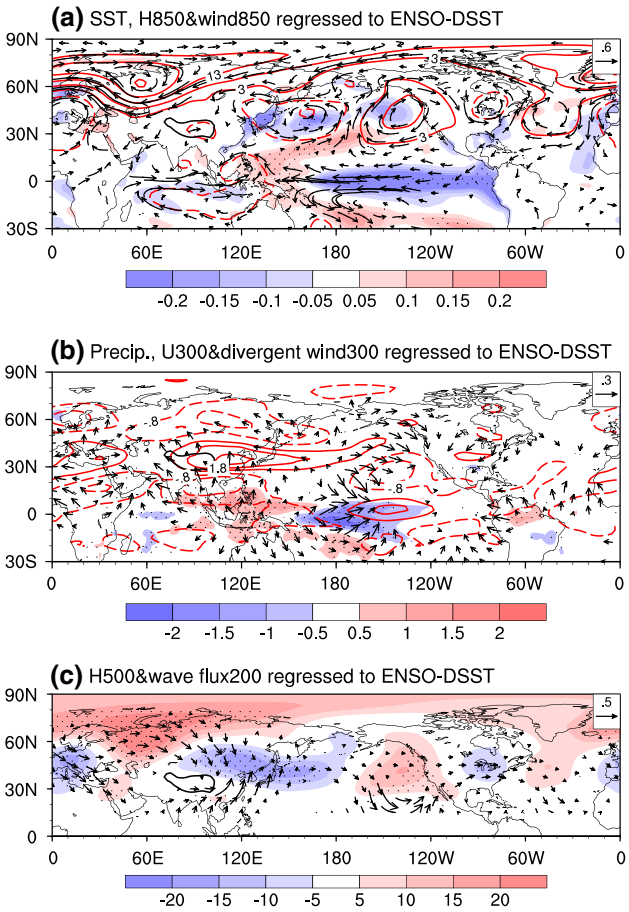

Fig. 7 Winter circulation anomalies associated with the autumn ENSO-DSST predictor. **a** Regressed winter H850 (*contours*; gpm), 850 hPa wind (*vectors*; m s^{-1}) and SST (*shaded*; °C) anomalies with reference to autumn ENSO-DSST predictor. The contour interval is 4 gpm; positive (negative) contours are *solid* (*dashed*) and zero contour is omitted. **b** Same as (**a**) but for the precipitation anomalies (*shaded*; mm/day), 300 hPa zonal wind (*contours*; m s^{-1}; the contour interval is 1 m s^{-1}) and 300 hPa divergent wind (*vectors*; m s^{-1}) anomalies. **c** Same as (**a**) but for the 500 hPa geopotential height (*shaded*; gpm) anomalies and 200 hPa wave activity flux (*vectors*; m^2 s^{-2}). *Dots* in (**a**–**c**) indicate region with regressed anomalies of SST, precipitation, and 500 hPa geopotential height significant at 95 % confidence level

anomaly over East Asia during SON tends to persist with the center slightly migrating northeastward from (35°N, 110°E) to (45°N, 120°E). The persistence and migration are accompanied by the persistence of the East Asian surface air cooling (Fig. 5a) and a cooling tendency across autumn season (Fig. 5b). The EA-H500 predictor signifies the East Asian trough deepening in the ensuing winter. The strengthened East Asian trough can lead to cold winters in East Asia.

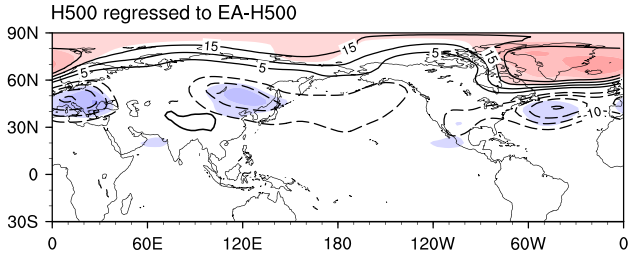

Fig. 8 Regressed winter (DJF) 500 hPa geopotential height (*contour*; gpm) anomalies with reference to the autumn EA-H500 predictor. The contour interval is 5 gpm, and zero contour is omitted. *Light* and *heavy color shadings* indicate the regressed anomalies significant at 95 and 99 % confidence level, respectively

6 Estimation of the predictability of NECD

In order to estimate potential predictability, we establish P-E prediction models with stepwise regression using the data from 1973 to 2013. All three predictors are selected by Stepwise regression with an F-test at 95 % significance level. The prediction equation derived from the training period of 1973–2013 is 2.06 * ARC-SST − 1.64 * ENSO-DSST − 1.94 * EA-H500. The simulation skill for this period reaches 0.78 (Fig. 9a).

We also made a 41-year retrospective forecast. The prediction models were derived by using a suite of consecutive 38-year data (leaving 3 years data out around each target prediction year), and then apply the derived model to forecast the middle year of the three withheld years. We have calculated the cross-validated correlation skill for the entire period (41 years), which is 0.73 (Fig. 9b), indicating about 50 % of the total variance is potentially predictable. This demonstrates a substantial improvement over the current dynamical prediction skill.

The result shown in this section provides a practical estimate for the lower bound of the potential predictability. The result suggests that the frequency of the extreme cold events during winter in the core region of the East Asian winter monsoon is to a large extent predictable before the season begins. It also provides a promising tool for seasonal forecast of the frequency of the extreme events of winter monsoon, since the multi-model ensemble prediction of winter extremes over global land only obtained an average correlation skill of 0.28 (Eade et al. 2012).

7 Source of the predictability of the NECD

Why are extremely cold events over the TEA region to a large extent predictable? We find that the physical basis for such a prediction is essentially the same as that for prediction of the seasonal mean temperature. Strong supporting evidence is that over the TEA region the winter mean temperature and the area averaged extreme condition (the NECD) are highly correlated.

As shown in Fig. 10, the NECD and the winter mean temperature are nearly out of phase with a correlation coefficient of −0.92. Similar to the NECD, the winter mean temperature over TEA exhibits a tiny linear trend with a slope of 0.18 °C/decade, which is statistically insignificant according to Mann–Kendall test (Kendall 1975). Instead, a multi-decadal change is evident with a transition to warm state in the mid-1980s (Wang et al. 2009b) as well as a downward swing since early 2000s (Wang and Chen 2013). Previous studies have suggested a close relationship between seasonal mean and the number of extreme days, and the prediction skill in predicting NECD arises largely from the skill in predicting seasonal mean temperature anomaly (Hamilton et al. 2012; Collins et al. 2000). Our

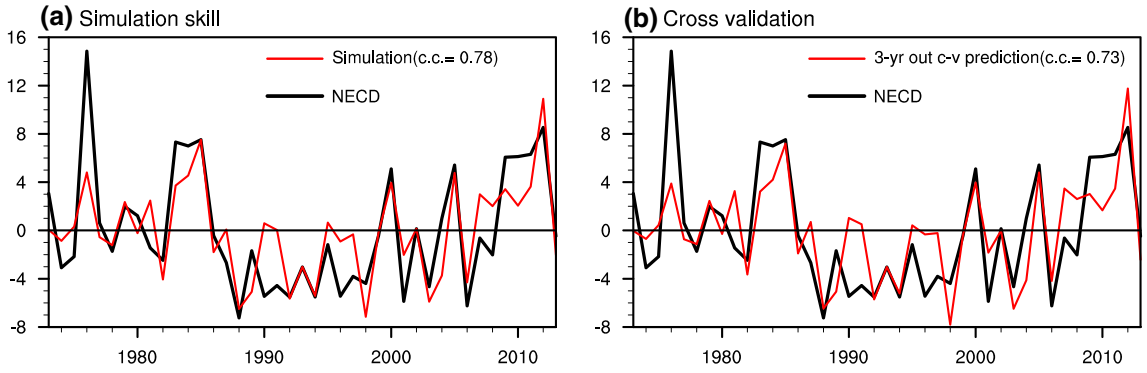

Fig. 9 Prediction skills of the physical-empirical (P-E) model. **a** The time series of observed NECD anomalies (*black line*) and the simulated NECD anomalies (*red line*). The data used for establishing the P-E model is from 1973 to 2013. The prediction is made at the end of November (0-month lead prediction). The simulated correlation skill for 1973–2013 is 0.78. **b** The time series of observed NECD (*black line*) and predicted NECD (*red line*) with cross-validation method obtained by taking 3-year out at each prediction step. The cross validated prediction skill for 1973–2013 is 0.73

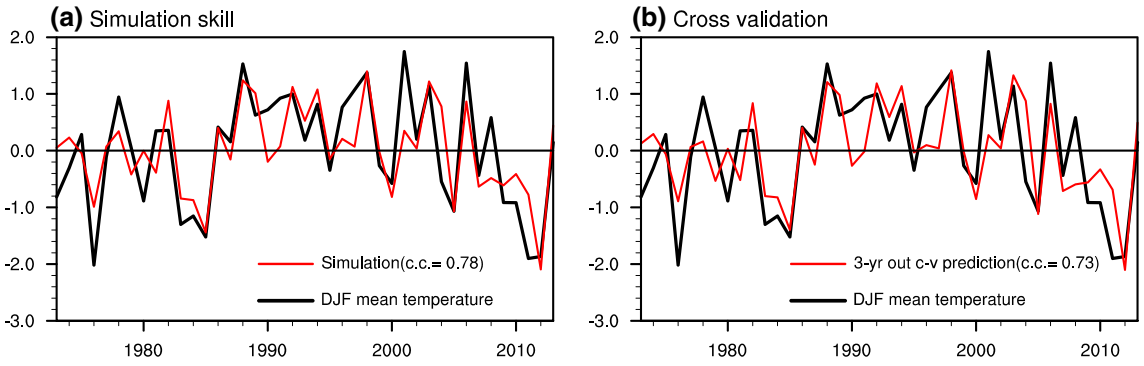

Fig. 10 The same as Fig. 9 except for the winter mean temperature over TEA

results are consistent with and confirmed the previous findings in the TEA region. The high correlation between winter mean temperature and NECD ($r = -0.92$) is very likely a result of a shift in the distribution of the daily temperature rather than a change of the shape of probability density function (Hamilton et al. 2012).

We have developed another suite of P-E models for prediction of winter mean temperature using the same procedure as that used to derive the P-E models for NECD. The correlation maps between the predictor fields and winter mean temperature resemble closely to those shown in Fig. 5 (figures not shown). Hence we used the same three predictors that were used to predict NECD (Table 1) to establish the P-E models for forecasting the winter mean temperature in TEA. As shown in Fig. 10b, the cross-validated correlation skill for winter mean temperature is 0.73 for the same 41-year period, similar to the prediction skill for NECD.

The shared sources of predictability between the ECD and the seasonal mean temperature at TEA suggest that the source of predictability of ECD is the same as the seasonal mean temperature, i.e., primarily rooted in the lower boundary anomalies over the ocean and land surface.

8 Concluding remarks

We have shown that the current dynamical models exhibit limited prediction skill for the winter mean temperature over the temperate East Asia (30°–50°N, 110°–140°E), the core region of the world strongest winter monsoon (Fig. 1). This motivated us to use Physics-based empirical (P-E) models to explore the source and limit of the seasonal predictability of the number of extremely cold days (NECD) averaged over temperate East Asia. The term "extremely cold" here is defined by the 10th percentile of the daily mean temperature at each 2.5° × 2.5° lat-long grid and in each winter month from December to the next February.

We find that the sources of the predictability for the NECD is essentially the same as those for the winter mean temperature over the same region, i.e., the anomalous lower boundary forcing from the ocean and land surface. The predictability is primarily rooted in three persistent processes from autumn to winter: developing ENSO, SST anomalies in Eurasian Arctic Ocean (Barents Sea-Kara Sea-Laptev Sea), and the East Asian continental cooling/warming. The plausible linkages between the three predictors in autumn and the winter NECD are discussed in Sect. 5.2.

We have shown that about 50 % of the total variance of the winter NECD over the core region of East Asian winter monsoon is predictable by using a P-E model with three physical consequential predictors. The cross-validated correlation skill reaches 0.73 for the 41-year period of 1973–2013. This practical prediction skill provides an estimate for the lower bound of the predictability of the NECD. This also suggests that dynamical models have large room to improve their prediction skills. Meanwhile the interdecadal change in ENSO-EAWM relationship is also noteworthy (Wang et al. 2008) and may influence the predictability of NECD.

The results obtained in this study are insensitive to definition of the ECD. We have compared the ECDs defined by the threshold at 20th percentile. The numbers of ECDs with 20th percentile threshold double that of the 10th percentile ECDs, but the two time series are extremely well correlated ($r = 0.98$) (Fig. 3). The simulation equation in Table 1 is based on 41 years period, and the simulation equation is sensitive to the simulation period, probably due to secular changes of relationship between predictand and predictors.

A surprising finding of the present study is that the 500 hPa height anomaly over northern and eastern Asia exhibits persistence from autumn to winter (Figs. 4c, 5c) so that the autumn anomaly can be used as a predictor for winter NECD. Since chaotic atmospheric circulation does not have long "memory" on seasonal time scale, it is curious how this persistence could occur. We note that the

500 hPa height anomalies are coherently coupled with land surface temperature anomalies. This coherent variation may mean a positive feedback between the surface cooling and the enhanced East Asian trough. On one hand, the surface cooling may lower the 500 hPa height and strengthen the EA trough. On the other hand, the enhanced EA trough may reinforce the cold advection behind the trough and promote cold surge to East Asia. This hypothesis needs further verification through numerical experiments. In general, the mechanism of the quasi-stationary negative anomalies at 500 hPa and its maintenance from autumn to winter need further exploration. Furthermore, the interpretations of the lead–lag linkages between the three predictors and predictand offered in Sect. 5.2 should be considered as hypotheses that aim to stimulate further study, especially in terms numerical experiments.

An interesting result is that over the core region of EAWM the frequency of extreme cold events and winter mean temperature have no significant trend but exhibit pronounced interdecadal fluctuation with two sharp transition around the mid-1980s and the early 2000s during the recent 41 years. That means, the global warming signal did not add a significant additional source of predictability to extreme event forecast. However, what causes this interdecadal variation calls for further investigation.

This finding that the extreme cold events share the same sources of predictability with the winter mean temperature has important ramification in the sense that forecast of seasonal mean temperature can provide critical information on the statistical properties of the temperature extremes. This is the case in winter temperature but likely valid for summer and other seasons too. To what extent this is the case for the extreme precipitation events remain to be explored.

Seasonal prediction of NECD using P-E model provides better prediction skills than those using UK Met Office seasonal forecasting models as analyzed by Eade et al. (2012). Moreover, although the Physics-based Empirical models have been successfully applied in Indian/Asian monsoon seasonal rainfall predictions, the P-E model for wintertime NECD/mean temperature prediction study is a new endeavour. The physical mechanisms we proposed for P-E model also provide good basis to evaluate current dynamical models' performances and for stimulating further numerical studies.

Acknowledgments This work has been supported by the Atmosphere-Ocean Research Center sponsored by the Nanjing University of Information Science and Technology and University of Hawaii. BW acknowledges the support provided by National Research Foundation (NRF) of Korea through a Global Research Laboratory (GRL) grant of the Korean Ministry of Education, Science and Technology (MEST, #2011-0021927). The authors thank Dr. So-Young Yim for discussing EAWM prediction issues. This is the SOEST publication 9662, IPRC publication 1202, and ESMC publication 115.

References

Arguez A et al (2012) NOAA's 1981–2010 U.S. climate normals: an overview. Bull Am Meteorol Soc 93:1687–1697

Barnston AG, Livezey RE (1987) Classification, seasonality and persistence of low-frequency atmospheric circulation patterns. Mon Weather Rev 115:1083–1126

Chang C-P, Wang Z, Hendon H (2006) The Asian winter monsoon. In: Wang B (ed) The Asian monsoon. Springer, Berlin, pp 89–127

Clark MP, Serreze MC (2000) Effects of variations in East Asian snow cover on modulating atmospheric circulation over the North Pacific Ocean. J Clim 13:3700–3710

Collins D, Della-Marta P, Plummer N, Trewin B (2000) Trends in annual frequencies of extreme temperature events in Australia. Aust Meteorol Mag 49:277–292

Eade R, Hamilton E, Smith DM, Graham RJ, Scaife AA (2012) Forecasting the number of extreme daily events out to a decade ahead. J Geophys Res Atmos 117:D21110. doi:10.1029/ 2012JD018015

Frich P, Alexander LV, Della-Marta P, Gleason B, Haylock M, Tank AMGK, Peterson T (2002) Observed coherent changes in climatic extremes during the second half of the twentieth century. Clim Res 19:193–212

Gong G, Entekhabi D, Cohen J (2002) A large-ensemble model study of the wintertime AO–NAO and the role of interannual snow perturbations. J Clim 15:3488–3499

Hamilton E, Eade R, Graham RJ, Scaife AA, Smith DM, Maidens A, MacLachlan C (2012) Forecasting the number of extreme daily events on seasonal timescales. J Geophys Res Atmos 117:D03114. doi:10.1029/2011JD016541

Honda M, Inoue J, Yamane S (2009) Influence of low Arctic sea-ice minima on anomalously cold Eurasian winters. Geophys Res Lett 36:L08707. doi:10.1029/2008GL037079

Huffman GJ, Bolvin DT (2013) GPCP version 2.2 SG combined precipitation data set documentation. NASA, pp 46. https://www.google.com.hk/url?sa=t&rct=j&q=&esrc=s&source=web&cd=2&cad=rja&uact=8&ved=0ahUKEwi_8f6m3bjNAhWIQI8KHWyXDAcQFggsMAE&url=%66%74%70%3a%2f%2f%70%72%65%63%69%70%2e%67%73%66%63%2e%6e%61%73%61%2e%67%6f%76%2f%70%75%62%2f%67%70%63%70%2d%76%32%2e%32%2f%64%6f%63%2f%56%32%2e%32%5f%64%6f%63%2e%70%64%66-&usg=AFQjCNGnCxS9cOJsr5XbfLsvbG-MgdelyQ

Jhun J-G, Lee E-J (2004) A new East Asian winter monsoon index and associated characteristics of the winter monsoon. J Clim 17:711–726

Kalnay E et al (1996) The NCEP/NCAR 40-year reanalysis project. Bull Am Meteorol Soc 77:437–471

Kendall MG (1975) Rank correlation methods, 4th edn. Charles Griffin, San Francisco

Klein Tank AMG, Zwiers FW, Zhang X (2009) Guidelines on analysis of extremes in a changing climate in support of informed decisions for adaptation. World Meteorol Organ 15:14–17

Kug J-S, Jeong J-H, Jang Y-S, Kim B-M, Folland CK, Min S-K, Son S-W (2015) Two distinct influences of Arctic warming on cold winters over North America and East Asia. Nat Geosci 8:759–762

Lee J-Y, Lee S-S, Wang B, Ha K-J, Jhun J-G (2013) Seasonal prediction and predictability of the Asian winter temperature variability. Clim Dyn 41:573–587

Li J, Wang B (2015) How predictable is the anomaly pattern of the Indian summer rainfall? Clim Dyn 46:2847–2861

Liu Y, Wang L, Zhou W, Chen W (2014) Three Eurasian teleconnection patterns: spatial structures, temporal variability, and associated winter climate anomalies. Clim Dyn 42:2817–2839

Luo X, Zhang Y (2015) The linkage between upper-level jet streams over East Asia and East Asian winter monsoon variability. J Clim 28:9013–9028

Mann HB (1945) Nonparametric tests against trend. Econom J Econom Soc 13:245–259

Michaelsen J (1987) Cross-validation in statistical climate forecast models. J Climate Appl Meteorol 26:1589–1600

Pepler AS, Díaz LB, Prodhomme C, Doblas-Reyes FJ, Kumar A (2015) The ability of a multi-model seasonal forecasting ensemble to forecast the frequency of warm, cold and wet extremes. Weather Clim Extremes 9:68–77

Smith TM, Reynolds RW, Peterson TC, Lawrimore J (2008) Improvements to NOAA's historical merged land–ocean surface temperature analysis (1880–2006). J Clim 21:2283–2296

Thompson DWJ, Wallace JM (1998) The Arctic oscillation signature in the wintertime geopotential height and temperature fields. Geophys Res Lett 25:1297–1300

Wang L, Chen W (2013) The East Asian winter monsoon: re-amplification in the mid-2000s. Chin Sci Bull 59:430–436

Wang L, Chen W (2014) An intensity index for the East Asian winter monsoon. J Clim 27:2361–2374

Wang B, Wu R, Fu X (2000) Pacific-East Asian teleconnection: how does ENSO affect East Asian climate? J Clim 13:1517–1536

Wang L, Chen W, Huang R (2008) Interdecadal modulation of PDO on the impact of ENSO on the east Asian winter monsoon. Geophys Res Lett 35:L20702

Wang B et al (2009a) Advance and prospectus of seasonal prediction: assessment of the APCC/CliPAS 14-model ensemble retrospective seasonal prediction (1980–2004). Clim Dyn 33:93–117

Wang L, Huang R, Gu L, Chen W, Kang L (2009b) Interdecadal variations of the East Asian winter monsoon and their association with quasi-stationary planetary wave activity. J Clim 22:4860–4872

Wang B, Wu Z, Chang C-P, Liu J, Li J, Zhou T (2010) Another look at interannual-to-interdecadal variations of the East Asian winter monsoon: the northern and southern temperature modes. J Clim 23:1495–1512

Wang B, Xiang B, Li J, Webster PJ, Rajeevan MN, Liu J, Ha KJ (2015) Rethinking Indian monsoon rainfall prediction in the context of recent global warming. Nat Commun 6:7154. doi:10.1038/ncomms8154

Watanabe M (2004) Asian jet waveguide and a downstream extension of the North Atlantic Oscillation. J Clim 17:4674–4691

Watanabe M, Nitta T (1999) Decadal changes in the atmospheric circulation and associated surface climate variations in the Northern Hemisphere winter. J Clim 12:494–510

Weisheimer A et al (2009) ENSEMBLES: a new multi-model ensemble for seasonal-to-annual predictions—skill and progress beyond DEMETER in forecasting tropical Pacific SSTs. Geophys Res Lett 36:L21711

Xing W, Wang B, Yim SY (2014) Peak-summer East Asian rainfall predictability and prediction part I: Southeast Asia. Clim Dyn. 47:1–13. doi:10.1007/s00382-014-2385-0

Yim S-Y, Wang B, Xing W (2014) Prediction of early summer rainfall over South China by a physical–empirical model. Clim Dyn 43:1883–1891

Zhang X, Yang F (2004) RClimDex (1.0) user manual. http://etccdi.pacificclimate.org/RClimDex/RClimDexUserManual.doc

Zhang R, Sumi A, Kimoto M (1996) Impact of El Niño on the East Asian Monsoon: a diagnostic study of the '86/87 and '91/92 events. J Meteorol Soc Jpn Ser II 74:49–62

Zhang X et al (2011) Indices for monitoring changes in extremes based on daily temperature and precipitation data. Wiley Interdiscip Rev Clim Change 2:851–870